A Receding Horizon Control Approach for Re-Dispatching Stochastic Heterogeneous Resources Accounting for Grid and Battery Losses

Eleni Stai, *Member, IEEE*, Fabrizio Sossan, *Member, IEEE*, Emil Namor, *Student Member, IEEE*, Jean-Yves Le Boudec, *Fellow, IEEE*, Mario Paolone, *Senior Member, IEEE*

***Abstract*—In this paper, we propose a re-dispatching scheme for radial distribution grids hosting Distributed Energy Resources (DERs) and batteries. The proposed scheme applies a Receding Horizon Control (RHC) over the CoDistFlow algorithm. CoDistFlow handles stochastic DERs and prosumers uncertainties via scenario-based optimization and the non-convexity of the AC Optimal Power Flow by iteratively solving suitably defined convex problems until convergence. RHC is applied for re-dispatching over regular time intervals using updated information (batteries state-of-energy, updated prosumption forecasts/scenarios). We perform numerical evaluations based on real-data, obtained on a real Swiss grid characterized by a large connection of stochastic DERs. We show that by re-dispatching via RHC, the daily dispatch tracking error can reduce more than 80%, while when re-dispatch becomes more frequent, it can be eliminated. In addition, we show that the daily dispatch tracking error reduction is much higher when re-dispatching in presence of larger batteries capacities. Finally, we study the computational complexity issues, as well as the efficiency of CoDistFlow for incorporating the grid/batteries losses.**

***Index Terms*—Dispatch plan; re-dispatch; intra-day; optimal power flow; grid losses; battery models; scenario-based;**

I. Introduction & Contributions

The joint dispatch of Distributed Energy Resources (DERs) and batteries allows for achieving (i) less costly balancing of load/generation during real-time operation [1], [2], [3], (ii) peak shaving [4], and (iii) voltage and ampacity constraints' satisfaction in local grids [5]. For a distribution grid with DERs and batteries, one approach is to commit with the day-ahead market a dispatch plan at the Point of Common Coupling (PCC) with the main grid, as well as computing appropriate battery setpoints, by solving an AC Optimal Power Flow (AC OPF) that considers the uncertainties of the prosumption, the grid/battery losses and the grid constraints [6]. Then, a real-time control algorithm re-computes the battery power in order to follow the dispatch plan based on the realization of the uncertain resources ([7], [8]).

However, when tracking a day-ahead dispatch plan during operation, (i) there may exist better forecasts for the remaining part of the day, and/or (ii) the realization might have not been close to the predicted day-ahead scenarios, leading to situations of depleted flexibility in the batteries. In this context, it is key to perform intra-day re-dispatching, i.e., update the dispatch plan for the upcoming time horizons accounting for more recent information. Indeed, it is widely accepted that the progressive penetration of renewable generation in modern power systems increases the importance of intra-day re-dispatching in order to compress the scheduling and activation of the primary/secondary frequency control reserve.

We propose an intra-day re-dispatch scheme for distribution grids with DERs and batteries which applies Receding Horizon Control (RHC) over the CoDistFlow algorithm, which is introduced in [6]. CoDistFlow is an iterative OPF algorithm (details are given in Section V-A) that, at each dispatch period, computes the updated dispatch plan for the next time horizon. It applies scenario-based optimization for handling the uncertainty of DERs and loads. Compared to the robust and chance-constrained optimizations, the advantages of scenario-based optimization are: (i) proper modeling of the uncertainty of stochastic resources [9] (e.g., non-parametric), (ii) inclusion of general convex constraints, and (iii) possibility to account for any existing time correlations. In this work, the scenarios consist of forecasted time-series constructed based on historical and present knowledge; thus the nonanticipativity condition [10] is not violated.

RHC is applied for re-dispatching over regular time intervals using updated information, i.e., currently observed state-of-energy of batteries and/or updated prosumption forecast scenarios. RHC adds an extra degree of robustness to the scenario-based optimization since the control values are updated based on the latest observations available, which, in general, might be different than the forecasts used in the previous time steps. Our method appropriately accounts for computational complexity issues that impact the possible time of commiting the updated dispatch plan (see in Section V). Finally, we model the internal losses of the grid-connected battery systems using equivalent lossy lines integrated in the power flow model [6], and we adopt an accurate representation of batteries' power-electronic's-converter apparent power constraints. To the best of our knowledge this is the most realistic model of battery losses in the literature.

CoDistFlow is chosen as the most suitable method for our setting. Specifically, to the best of our knowledge, CoDistFlow is the only algorithm in the literature for solving a scenario-based AC OPF while providing a solution that satisfies the exact power flow equations and the exact grid security constraints. It is shown in [6] that existing AC OPF relaxation methods yielding exact solutions, e.g., [11], [12], do not apply in case of scenario-based optimization. In addition, in [6], it is shown that the commonly applied sequential linearization

The authors are with the École Polytechnique Fédérale de Lausanne (EPFL), Lausanne 1015, Switzerland. E-mails: {eleni.stai, fabrizio.sossan, emil.namor, jean-yves.leboudec, mario.paolone}@epfl.ch

of the power flow equations with sensitivity coefficients may have a slow convergence and may lead to a non-optimal solution. Moreover, CoDistFlow is computationally efficient for being integrated in an RHC framework, as it converges in few iterations [6].

This paper investigates the importance of re-dispatching and quantifies it by introducing appropriate measures based on existing reserve markets and by evaluations on real datasets. To the best of our knowledge, the proposed RHC over CoDistFlow is the only method in the literature that re-dispatches the operation of a distribution grid in a complete setting, since, (i) it considers distributed batteries and DERs, (ii) it handles the uncertainty via scenario-based optimization, (iii) it obtains solutions that satisfy the exact power flow equations and the exact grid constraints, (iv) it accounts for an accurate model of battery losses and constraints.

We perform extensive numerical evaluations on a real-life distribution system in Switzerland composed by 34 buses and using real data to construct the scenarios. By solving large scale optimization problems, we show that by re-dispatching via RHC, the error in tracking the dispatch plan, as well as the corresponding energy cost, reduce significantly. Moreover, these costs further reduce as re-dispatching becomes more frequent. We study the performance of RHC over CoDistFlow with respect to the number of scenarios and battery capacities. Finally, we indicate the importance of incorporating CoDistFlow to efficiently account for the grid/batteries losses.

The rest of the paper is organized as follows. Section II summarizes the related literature. Section III describes the system model and the assumptions. Section IV formulates the problem and Section V proposes the RHC over CoDistFlow scheme. Section VI presents the evaluation results and finally Section VII concludes the paper.

II. Related Works on Re-dispatching

Re-dispatch strategies for intra-day markets and real-time operation of power grids have been extensively discussed in the literature. In [13], the Authors propose an intra-day multi-period energy and reserve pre-dispatch model and a real-time single time-slot re-dispatch model. Contrary to our approach, neither prosumption uncertainty is considered, nor the adaptation of previous decisions to the revealed prosumption and the updated forecasts. The work in [14] performs single time-slot re-dispatching (thus without an MPC strategy) without considering energy storage. For the solution, the prosumption uncertainty is handled via chance-constraints on a second order cone programming OPF. The chance constraints are approximated based on a known parametric probability distribution of the uncertainty, contrary to our proposed approach that uses scenario-based optimization.

MPC-based grid operational control schemes have been also examined, e.g., [10], [15], [16], [17], [18], [19]. In particular, in [15], RHC and scenario-based optimization are applied for the operational control of islanded microgrids using the well known DC approximation of the power flow and without accounting for energy storage losses. In [10], a real-time RHC-based power dispatch scheme is proposed for a grid with DERs and energy storage using scenario-based optimization. In [16], the coordinated operation of wind farms and energy storage is studied, by applying a 4 hours-ahead RHC scheme and wind power forecast scenarios. The work in [17] applies RHC to re-dispatch a battery storage system coupled to PV generation using point forecasts for the PV and the load. Works [18] and [19] propose RHC for operating a microgrid with the aim of minimizing its operating costs. [18] applies scenario-based optimization whereas [19] replaces the uncertain quantities with point forecasts. It is shown that the operating cost and the number of violations of the storage capacity constraints are considerably reduced if using RHC compared to the solution of a day-ahead problem. All the mentioned works [10], [16], [17], [18], [19], contrary to our approach, do not model the grid and the associated operational voltage/current constraints.

Compared to the above-listed works, our approach efficiently re-dispatches the operation of a distribution grid with distributed battery energy storage and DERs while appropriately accounting for uncertainties, and accurately modeling the grid constraints and the batteries constraints and losses.

III. System Model & Nomenclature

We consider a balanced and transposed radial distribution grid. The PCC is at index 0 and is assumed to be the only slack bus. Distribution lines and, in general, branches are represented by their single-phase direct sequence equivalent exact π models (Fig. 1(a)). Note that the same model can be used to represent other devices connected between nodes (e.g., series voltage regulating transformers). This modeling approach is particularly suitable for underground cables that are used especially in urban contexts. The indices of buses (except the PCC) and of lines lie in $\{1, 2, ..., N\}$. The node at the top of line ℓ closer to the PCC, is denoted as $\mathrm{up}(\ell)$, and the node at the bottom as ℓ (Fig. 1(a)). We assume that the PCC lies at the top of line $\ell = 1$. The index of time is $t \in \{0, 1, ..., T-1\}$, and the index of scenarios is $d \in \{1, 2, ..., D\}$. Each time interval has a duration of Δt (in hours). The $N \times N$ matrix $\mathbf{G}$ is the adjacency matrix of the oriented graph of the network excluding the PCC, i.e., $\mathbf{G}_{k,\ell} = 1$ for two buses $k, \ell \neq 0$, if $k = \mathrm{up}(\ell)$, otherwise $\mathbf{G}_{k,\ell} = 0$. We use $|.|$, $\|.\|$ for the absolute value and the Euclidean norm, respectively.

On each line ℓ (Fig. 1(a)), let (i) $S^d_\ell(t) = P^d_\ell(t) + \jmath Q^d_\ell(t)$ be the direct sequence complex power fed from the bus $\mathrm{up}(\ell)$, (ii) $z_\ell = r_\ell + \jmath x_\ell$ and b_ℓ be the direct sequence longitudinal impedance and shunt susceptance of the branch ℓ, (iii) $f^d_\ell(t)$ be the square magnitude of the direct sequence current flowing through z_ℓ, and (iv) $i^d_\ell(t)$ ($i^{b,d}_\ell(t)$) be the current at the top (bottom) of branch ℓ. $\overline{I}_\ell$ is the ampacity limit of branch ℓ.

On each bus/node ℓ (Fig. 1(a)), (i) $v^d_\ell(t)$ is the square magnitude of the direct sequence voltage, (ii) $\underline{v}$, $\overline{v}$ are lower and upper bounds of $v^d_\ell(t)$, i.e., $\underline{v}^2 \leq v^d_\ell(t) \leq \overline{v}^2$, (ii) $s^d_\ell(t) = p^d_\ell(t) + \jmath q^d_\ell(t)$ is the complex power injection without the battery power injections ($p^d_\ell(t) > 0$, $q^d_\ell(t) > 0$ indicate consumption). Also, $S^{DP}(t) = P^{DP}(t) + \jmath Q^{DP}(t)$ stands for the dispatched complex power at PCC, at time t. At PCC the voltage is assumed fixed, $v^d_0(t) = 1$ pu, $\forall t, d$.

Each battery, along with its power conversion devices, is represented by a lossy equivalent power source (Fig. 1(b)) [6]. For each battery connected to bus ℓ, a new virtual node is added and connects to this bus via a virtual purely resistive

line. If there exist N_B batteries in the grid, the total number of buses increases to $N + N_B$ and the admittance matrix of the grid is appropriately updated. The battery model is characterized by the resistance of the newly added virtual line (Fig. 1(b)) that can be assessed experimentally as in [6]. Then, (i) the battery losses are equal to the active power losses of this resistive line, and (ii) the state-of-energy (SoE) is equal to the one of a lossless battery, with same capacity and rated power connected to the virtual node. As the reactive power is entirely generated (or absorbed) by the battery inverter, there are no losses on the virtual line due to the battery reactive power (see Fig. 1(b)). For a battery at virtual node ℓ, let (i) $\text{SoE}^d_\ell(t)$ be its state-of-energy at time t and for scenario d, (ii) $\overline{\text{SoE}}_{B,\ell}$ be its energy capacity, i.e., $0 \leq \text{SoE}^d_{B,\ell}(t) \leq \overline{\text{SoE}}_{B,\ell}$, (iii) $p^d_{B,\ell}(t)$ be the charging ($p^d_{B,\ell}(t) \geq 0$) or discharging ($p^d_{B,\ell}(t) \leq 0$) power at time t and scenario d, without including the battery losses, (iii) $q^d_{B,\ell}(t)$ be the reactive power, (iv) $s_{B,\ell}(t) = p^d_{B,\ell}(t) + \jmath q^d_{B,\ell}(t)$ and (v) $s^R_{B,\ell}$ be its rated power. Note that, we impose neither ampacity constraints to the virtual line, nor voltage constraints at the virtual node, since both are only part of the battery model. Finally, after representing all batteries with their models, the battery capacity is non-zero only at the virtual nodes i.e., those within the set $\{N+1, ..., N+N_B\}$.

We define $P^d(t) = [P^d_1(t), P^d_2(t), ..., P^d_N(t)]^T$ the active power flow values for all lines. Similarly, we define the vectors: $Q^d(t)$ for the reactive power, $v^d(t)$ for buses' voltages (square magnitude) and $p^d(t)$, $q^d(t)$, $p^d_B(t)$, $q^d_B(t)$, for the node active and reactive prosumption injections and battery active and reactive power values, respectively. In Section V, for the needs of CoDistFlow, we use the correction terms $\hat{p}^d_\ell(t)$, $\hat{q}^d_\ell(t)$, $\hat{v}^d_\ell(t)$ and the approximation terms $\tilde{v}^d_\ell(t)$ (for line ℓ, scenario d and time t). Furthermore, $\hat{P}^d(t) = [\hat{p}^d_1(t), ..., \hat{p}^d_N(t)]^T$, $\hat{Q}^d(t) = [\hat{q}^d_1(t), ..., \hat{q}^d_N(t)]^T$, $\hat{V}^d(t) = [\hat{v}^d_1(t), ..., \hat{v}^d_N(t)]^T$, and $\tilde{V}(t,d) = [\tilde{v}^d_1(t), ..., \tilde{v}^d_N(t)]^T$. We introduce more compact notations for the electrical state of the grid $E(t,d)$, the corrections $C(t,d)$, the load injections $s(t,d)$ and the battery power values $s_B(t,d)$, as $E(t,d) = [P^d(t);\ Q^d(t);\ v^d(t)]$, $C(t,d) = [\hat{P}^d(t);\ \hat{Q}^d(t);\ \hat{V}^d(t)]$, $s(t,d) = [p^d(t);\ q^d(t)]$, $s_B(t,d) = [p^d_B(t);\ q^d_B(t)]$.

To conclude, some collective notation: S denotes complex power for all lines (top/bottom), scenarios and times, v denotes voltage square magnitude for all buses, scenarios and times, S^{DP} defines the dispatched complex power for all times, and f denotes the square magnitude currents flowing through the longitudinal impedances for all lines, scenarios and times.

IV. Problem Formulation

We solve, at regular time intervals, a scenario-based AC OPF for a radial distribution network with stochastic renewable energy sources and battery storage. We consider the following constraints.

a) Power Flow Equations defined $\forall t, d$, line ℓ:

$$P^d_\ell(t) = \sum_{k:\mathbf{G}_{\ell k}=1} P^d_k(t) + p^d_\ell(t) + p^d_{B,\ell}(t) + r_\ell f^d_\ell(t), \quad (1)$$

$$Q^d_\ell(t) = \sum_{k:\mathbf{G}_{\ell k}=1} Q^d_k(t) + q^d_\ell(t) + q^d_{B,\ell}(t) - (v^d_{\text{up}(\ell)}(t) + v^d_\ell(t))b_\ell/2 + x_\ell f^d_\ell(t), \quad (2)$$

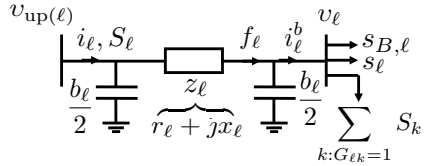

(a) π model of a line.

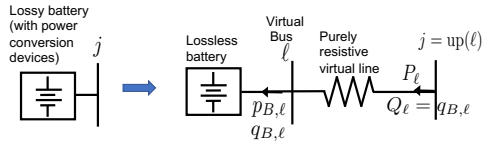

(b) Battery model.

Fig. 1: Line (a) and Battery (b) models.

$$f^d_\ell(t) = \left\| S^d_\ell(t) + j\frac{v^d_{\text{up}(\ell)}(t) b_\ell}{2} \right\|^2 / v^d_{\text{up}(\ell)}(t). \quad (3)$$

b) Voltage Constraints, defined $\forall t, d$, bus ℓ:

$$v^d_\ell(t) = v^d_{\text{up}(\ell)}(t) - 2\Re\left\{ z^*_\ell \left(S^d_\ell(t) + j v^d_{\text{up}(\ell)}(t)\frac{b_\ell}{2} \right) \right\} + \|z_\ell\|^2 f^d_\ell(t), \quad (4)$$

$$v^d_{\text{up}(1)}(t) = 1,\ \underline{v}^2 \leq v^d_\ell(t) \leq \overline{v}^2. \quad (5)$$

c) Ampacity Constraints, defined $\forall t, d$, line ℓ:

$$\Re\{i^d_\ell(t)\} = \frac{P^d_\ell(t)}{\sqrt{v^d_{\text{up}(\ell)}(t)}}, \quad \Im\{i^d_\ell(t)\} = \frac{Q^d_\ell(t)}{\sqrt{v^d_{\text{up}(\ell)}(t)}}, \quad (6)$$

$$\Re\{i^{b,d}_\ell(t)\} = \left(P^d_\ell(t) - r_\ell f^d_\ell(t)\right)/\sqrt{v^d_\ell(t)}, \quad (7)$$

$$\Im\{i^{b,d}_\ell(t)\} = \left(Q^d_\ell(t) - x_\ell f^d_\ell(t)\right)/\sqrt{v^d_\ell(t)} + \left(v^d_{\text{up}(\ell)}(t) + v^d_\ell(t)\right) b_\ell / \left(2\sqrt{v^d_\ell(t)}\right), \quad (8)$$

$$\|i^d_\ell(t)\| \leq \overline{I}_\ell, \|i^{b,d}_\ell(t)\| \leq \overline{I}_\ell. \quad (9)$$

d) Battery Constraints, defined $\forall t, d$, bus ℓ:

$$\text{SoE}^d_{B,\ell}(t+1) = \text{SoE}^d_{B,\ell}(t) + p^d_{B,\ell}(t)\Delta t, \quad (10)$$

$$a_B \overline{\text{SoE}}_{B,\ell} \leq \text{SoE}^d_{B,\ell}(t) \leq (1-a_B)\overline{\text{SoE}}_{B,\ell}, \quad (11)$$

$$\left(P^d_\ell(t)\right)^2 + (q^d_{B,\ell}(t))^2 \leq (s^R_{B,\ell})^2, \quad (12)$$

$$\text{SoE}^d_{B,\ell}(0) = \text{SoE}^I_{B,\ell}, \quad (13)$$

where (i) $0 \leq a_B \leq 1$ is a constant parameter used to define a margin on the state-of-energy lower and upper bounds, and (ii) SoE^I_B is a vector with dimension $N+N_B$ and its element, $\text{SoE}^I_{B,\ell}$, is the given initial SoE of the battery at node ℓ.

The above set of constraints is non-convex due to the Eqs. (3) and (6)-(9). Note that the battery apparent power constraint of Eq. (12) does represent an improvement of the corresponding one in [6] when using the battery resistance model. Indeed, it considers the battery active power not at the virtual bus ℓ of the battery model, but, at the bus $\text{up}(\ell)$, i.e., including the battery losses.

We assume that the first scenario (i.e., scenario with index 1) consists of the point forecasts of the prosumption at each bus and time. The rest of the scenarios are constructed based on probabilistic forecasts as in [9] (see Section VI-A for details). All the scenarios are based on historical data and present

knowledge at the time the OPF is solved and thus the decisions taken are nonanticipative. In case that D attains a large value ($\gg 100$) and computational complexity issues emerge, then scenario reduction techniques can be applied, as e.g., in [6].

Next, we give the considered objective function,

$$\begin{aligned} & w_1 \sum_{d,t,\ell} \lambda_d \max\left(\underline{\mathrm{E}}_{B,\ell} - \mathrm{SoE}^d_{B,\ell}(t), 0, \mathrm{SoE}^d_{B,\ell}(t) - \overline{\mathrm{E}}_{B,\ell}\right) \\ & + w_2 \sum_{d,t} \lambda_d |Q^d_1(t)| + w_3 \sum_{d,t} \lambda_d |P^d_1(t)| + w_4 \sum_{d,t} \lambda_d P^d_1(t) \\ & + w_5 \sum_{d,t} \lambda_d \left(|P^d_1(t) - P^{DP}(t)| + |Q^d_1(t) - Q^{DP}(t)|\right) \\ & + w_6 \sum_{k,d,t} \lambda_d |\sum_{j,i\in\mathcal{I}_k} (p^d_{B,j}(t) + p^d_i(t) - p^1_i(t))|. \end{aligned} \tag{14}$$

The first objective penalizes the deviation of $\mathrm{SoE}^d_{B,\ell}(t)$ above $\overline{\mathrm{E}}_{B,\ell}$ and below $\underline{\mathrm{E}}_{B,\ell}$. The second objective minimizes the reactive power at the PCC ($|Q^d_1(t)|$) that serves the purpose of maximizing the power factor at the PCC. The third objective minimizes the active power exchanged with the upstream power grid. The fourth goal is to maximize the power export to the main grid. This objective also minimizes the sum of line losses, thus implicitly prioritizing batteries for each load, i.e., the battery that is closer to the load will be preferably used otherwise the losses will increase. Note that battery losses are handled similarly to the line losses; also being minimized through this objective. The fifth objective minimizes the error between the obtained dispatch plan and the optimal power at the PCC for every scenario. The sixth term explicitly prioritizes batteries for absorbing the uncertainty of specific loads, where $\mathcal{I}_k$ is a set of buses with battery j and buses with prosumption i. The individual objectives are weighted by the positive constants $w_i,\ i = 1, ..., 6$. Finally, the objective function is a weighted average over all scenarios, where the weight λ_d is the probability of occurrence of scenario d, with $\sum_d \lambda_d = 1$. The non-convex AC OPF is formulated as follows:

$$\min_{S, s_B, v, S^{DP}, f} (14), \quad s.t.\ \forall t, d, \ell,\ (1) - (13). \tag{15}$$

Our aim is to obtain updated trajectories for the dispatch plan, S^{DP}, and the battery power, s_B, by solving the non-convex problem (15) in an efficient way, repeatedly over regular intervals. Each time we solve (15) we should account for the currently observed values of the batteries' SoE and the updated prosumption scenarios in order to re-dispatch efficiently, i.e., compute an updated S^{DP} that adapts better to the current information than the previously computed one. To do so, we apply CoDistFlow [6] for solving the scenario-based non-convex problem (15), and RHC for re-dispatching.

V. Proposed Approach: RHC over CoDistFlow

Every $\Delta\tau$ (in hours), we solve (15) for a horizon length of T time intervals each of duration Δt, where we assume that $\Delta\tau/\Delta t$ is a positive integer. Specifically, we compute an updated dispatch plan at the PCC, S^{DP}, via (15) at times $\tau = \rho\frac{\Delta\tau}{\Delta t}$, with $\rho \in 0, 1, 2, 3, \cdots$ (see Algorithm 2). For large-scale problems (i.e., large values of the number of scenarios D, network size and horizon length T) as the ones considered in our evaluations, solving the non-convex problem (15) via CoDistFlow may require a non-negligible computational time. Assume that the required computational time is at most T_{fixed} time intervals, i.e., $T_{fixed}\Delta t$. Therefore, the computation performed at time τ will be completed at most at time $\tau + T_{fixed}$; thus, it is not be possible to guarantee committing before time $\tau + T_{fixed}$, the dispatch plan for the first T_{fixed} time intervals. To solve this issue, for the first T_{fixed} time intervals we commit the dispatch plan computed at $\tau - 1$ for the corresponding time intervals, assuming that $T > \frac{\Delta\tau}{\Delta t} + T_{fixed}$. Specifically, we define S^{DP}_{fixed} as a vector of length T_{fixed} with elements the dispatched complex power at $\tau - 1$ for the mentioned time intervals. Then, we add the constraint of Eq. (16) to account for this dispatch plan commitment when solving (15) at τ. To present our approach, we describe and adapt CoDistFlow [6] and then apply RHC.

A. CoDistFlow

CoDistFlow [6] consists of two modules, namely: Improved DistFlow (iDF) and Load Flow (LF). These two modules are applied sequentially and iteratively until convergence.

1) Improved DistFlow (iDF) and Load Flow (LF) Modules: The iDF module is given as $[S^{DP}, E', s_B] = \mathrm{iDF}(s, C, \tilde{V}, \mathrm{SoE}^I_B, S^{DP}_{fixed})$, where SoE^I_B collects the currently observed batteries SoE values, inserted as inputs to iDF, as initial ones for the computations. iDF solves a problem similar to (15), but, with the following differences. First, it introduces the constant correction terms $\hat{p}^d_\ell(t)$, $\hat{q}^d_\ell(t)$, $\hat{v}^d_\ell(t)$ that replace the variables $r_\ell f^d_\ell(t)$, $x_\ell f^d_\ell(t)$ and $\|z_\ell\|^2 f^d_\ell(t)$, respectively, in Eqs. (1)-(9). In addition, iDF introduces the constant approximation terms, $\tilde{v}^d_\ell(t)$, which replace the voltage magnitude variables, $\sqrt{v^d_\ell(t)}$, in Eqs. (6)-(9). Given constant values of the correction and approximation terms, C, $\tilde{V}$, and the above replacements, the problem (15) becomes convex and can be efficiently solved. Second, the problem solved by iDF has in addition the constraint (16), which is required to integrate CoDistFlow within the RHC framework. Its meaning is discussed above.

Fixed Dispatch Plan Constraints:

$$S^{DP}(0 : T_{fixed} - 1) = S^{DP}_{fixed}. \tag{16}$$

As mentioned above, iDF solves a convex OPF with constant correction and approximation terms. The values of the correction and approximation terms are computed/updated by the LF module, by solving a full AC load flow ((Eqs. (1)-(4))) for a specific time and scenario. The LF module is given as $[E(t,d), C(t,d), \tilde{V}(t,d)] = \mathrm{LF}(s_B(t,d), s(t,d))$. The batteries are also considered as PQ buses with injections computed by iDF at the previous iteration.

2) CoDistFlow: CoDistFlow is given in Algorithm 1. The superscript (k) denotes the iteration k of CoDistFlow and the index j in lines $7 - 10$ the j^{th} element of the corresponding vectors. According to [6], at convergence the obtained solution satisfies the exact (AC) power flow equations and the exact operational constraints (i.e., Eqs. (1)-(13)) within the tolerance bounds imposed by the convergence criterion, i.e., if CoDistFlow terminates at iteration k_1, the electrical states $E'^{(k_1)}$, $E^{(k_1)}$ (almost) coincide.

Algorithm 1: CoDistFlow $(S^{DP}, s_B) = CoDistFlow(s, \text{SoE}_B^I, S_{fixed}^{DP})$

$k = 0$; convergence $= false$;
$C^{(0)} = \mathbf{0}$; $\tilde{V}^{(0)} = \mathbf{1}$;
while *convergence* $= false$ **do**
  $[S^{DP,(k)}, E'^{(k)}, s_B^{(k)}] =$ iDF$(s, C^{(k)}, \tilde{V}^{(k)}, \text{SoE}_B^I, S_{fixed}^{DP})$;
  for *each time* t *and scenario* d **do**
    $[E^{(k)}(t,d), C^{(k+1)}(t,d), \tilde{V}^{(k+1)}(t,d)] =$ LF$(s_B^{(k)}(t,d), s(t,d))$;
  if $k \geq 1$ *and*
    $\sup_{j,d,t} \left| C_j^{(k+1)}(t,d) - C_j^{(k)}(t,d) \right| \leq \epsilon_c$ *and*
    $\sup_{j,d,t} \left| \tilde{V}_j^{(k+1)}(t,d) - \tilde{V}_j^{(k)}(t,d) \right| \leq \epsilon_v$ *and*
    $\sup_{j,d,t} \left| \Re\{s_{B,j}^{(k)}(t,d) - s_{B,j}^{(k-1)}(t,d)\} \right| \leq \epsilon_B$ *and*
    $\sup_{j,d,t} \left| \Im\{s_{B,j}^{(k)}(t,d) - s_{B,j}^{(k-1)}(t,d)\} \right| \leq \epsilon_B$
  then
    convergence $= true$;
  $k \leftarrow k + 1$;
return $S^{DP} \leftarrow S^{DP,(k-1)}$, $s_B \leftarrow s_B^{(k-1)}$;

B. RHC over CoDistFlow

We solve (15) via CoDistFlow every $\Delta\tau$, at time instants indicated by τ. We obtain the battery trajectories for all scenarios and the dispatch plan. We assume that between two re-dispatch instances (i.e., during $\Delta\tau$), a real-time algorithm is applied to decide the battery setpoints with the aim of following the committed dispatch plan, while each battery SoE is updated based on these decisions. The real-time control algorithm runs every Δt_r (in hours), with $\Delta t_r \leq \Delta t \leq \Delta\tau$, at time instants indicated by t_r, where $\Delta t / \Delta t_r$ is assumed a positive integer. Notice that at time τ, we compute $t_r = \tau \frac{\Delta t}{\Delta t_r}$. Fig. 2 illustrates the diverse times and scales, e.g., the times of computing and committing the dispatch plan based on Algorithm 2. Also, let $\text{SoE}_{B,\ell}^o(t_r)$ be the observed state-of-energy at bus ℓ and time t_r, and $\text{SoE}_B^o(t_r)$ be the vector with elements $\text{SoE}_{B,\ell}^o(t_r)$ for all buses (dimension $N + N_B$).

The RHC over CoDistFlow scheme is given in Algorithm 2. At time τ, CoDistFlow takes as inputs (i) s_τ which is defined similarly as s and stands for the updated prosumption scenarios for all buses at time τ; (ii) $\text{SoE}_B^o(\frac{\tau \Delta t}{\Delta t_r})$, which is the observed SoE at $\tau \Delta t$ and (iii) S_{fixed}^{DP}, defined above. CoDistFlow outputs S_τ^{DP}, i.e., the dispatch plan for time intervals $\{\tau, ..., \tau + T - 1\}$. CoDistFlow and the real-time control algorithm can start running in parallel, since the dispatch plan for the time intervals $\{\tau, ..., \tau + T_{fixed} - 1\}$ is known. When CoDistFlow finishes its computation (after T_{fixed} time intervals) the real-time control algorithm starts using the obtained S_τ^{DP} instead of S_{fixed}^{DP}. All other computations except CoDistFlow are assumed instantaneous. Finally, we consider that the SoE is observed before each re-dispatch at times τ and before each real-time battery control decision at times t_r; in this way we account for any uncertainties in the implementation of the real-time decisions by the batteries.

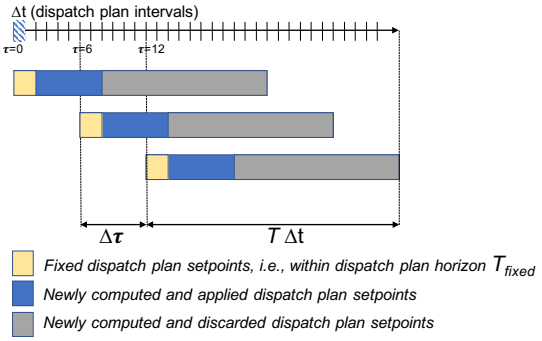

Fig. 2: Illustration of time intervals in the RHC over CoDistFlow scheme.

Algorithm 2: RHC over CoDistFlow

$\tau = 0$;, $t_r = 0$;
$\text{SoE}_B^o(0)$, S_{fixed}^{DP}, known;
while *true* **do**
  Observe $\text{SoE}_B^o(t_r)$;
  $s_\tau \leftarrow$ updated prosumption scenarios for time intervals $\{\tau, ..., \tau + T - 1\}$;
  $S_\tau^{DP} \leftarrow \emptyset$;
  At time t_r, run in parallel 1, 2:
  1. $(S_\tau^{DP}, s_B) = CoDistFlow(s_\tau, \text{SoE}_B^o(t_r), S_{fixed}^{DP})$;
  2. **while** $t_r < t_r + \frac{\tau \Delta t + \Delta_\tau}{\Delta t_r}$ **do**
    Compute $t_n = \left\lfloor \frac{t_r \Delta t_r - \tau \Delta t}{\Delta t} \right\rfloor$;
    Take real-time decisions using (i) $\text{SoE}_B^o(t_r)$ and (ii) $S_\tau^{DP}(t_n)$ if $S_\tau^{DP} \neq \emptyset$ or else $S_{fixed}^{DP}(t_n)$;
    Wait Δt_r; $t_r \leftarrow t_r + 1$;
  $S_{fixed}^{DP} \leftarrow S_\tau^{DP}(0 : T_{fixed} - 1)$;
  $\tau \leftarrow \tau + \frac{\Delta \tau}{\Delta t}$;

VI. Evaluation Results

We perform numerical evaluations and comparisons of the proposed RHC over CoDistFlow re-dispatch scheme. We study the impact of several factors on the re-dispatch performance and complexity, such as the battery size, the number of scenarios and the consideration of grid and battery losses. We set $\Delta t = \Delta t_r = 0.25$ h, $T = 96$, while $\Delta\tau$ varies. We compare re-dispatching via RHC over CoDistFlow, with a scheme that the dispatch plan is computed just before the day it is applied and it is not further updated intra-day. For the latter scheme, called "No Re-dispatch", we use the algorithms of Section V-B, but, we set $\Delta\tau = T = 96$. Thus, the problems solved every $\Delta\tau$ refer to completely disjoint time periods. RHC over CoDistFlow is indicated with "Re-dispatch".

The simulations are performed for a real Swiss grid, shown in Fig. 3. It consists of 34 buses, including the PCC. There is one battery connected to bus 1, with maximum apparent power 6 MW and capacity 3 MWh (three-phase), and one battery connected to bus 23 with the same characteristics. The buses 34 and 35 are virtual buses for the battery models. The max/min (magnitude) line impedance is $(0.34 + j0.24)/(0.025 + j0.01)$ Ω, the max/min shunt capacitance is $200.15/6.73$ μS and the max/min ampacity limit is $400/140$

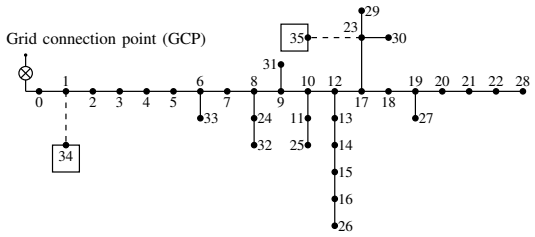

Fig. 3: Illustration of the real Swiss grid used for our numerical evaluations. The squares indicate nodes with batteries.

A. The power base is 25 MW and the voltage base is 21 kV. We set $\underline{v} = 0.9$ pu, $\overline{v} = 1.1$ pu, and that the initial SoE of all batteries is equal to 1 MWh, for all scenarios.

We apply $D = 80$ scenarios, except differently mentioned, created as described in Section VI-A. By choosing this D, we tried to account for as much detailed information of the uncertainty as possible while maintaining a manageable computational complexity. Note that we tackle large scale problems ($N = 36$, $T = 96$, $D = 80$ and several decision variables per node, time and scenario), with much larger dimensions than in the literature e.g., [15], [10], [18]. We use Matlab with the Yalmip toolbox and the Gurobi solver.

We introduce the following measures. The applied dispatch plan value at t_r based on our intra-day computations is equal to $P^{DP}\Big(\Big\lfloor (t_r\Delta t_r - \tau\Delta t)/\Delta t \Big\rfloor\Big)$. Let $P_1(t_r)$ be the realized power at PCC, at t_r, when the true prosumption is revealed and the battery power decisions are applied after being computed by the real-time control algorithm. The dispatch plan power error at t_r, denoted as DP_E, is defined as

$$DP_E(t_r) = P_1(t_r) - P^{DP}\Big(\Big\lfloor (t_r\Delta t_r - \tau\Delta t)/\Delta t \Big\rfloor\Big). \quad (17)$$

When $DP_E(t_r) = 0$, the dispatch plan can be followed at t_r. According to the energy market Fingrid [20], the dispatch plan error in terms of energy is defined per hour. Let us denote as $t_h \in \{0, 1, 2, ...\}$ the index of hours, and assuming that $1/\Delta t_r$ is an integer, we define:

$$DE_E(t_h) = \sum_{t_r = t_h/\Delta t_r}^{t_h/\Delta t_r + 1/\Delta t_r} DP_E(t_r)\Delta t_r. \quad (18)$$

When $DE_E(t_h) > 0$, the required energy at hour t_h exceeds the planned one and we need to pay up-regulation costs [20], at price χ^+. Similarly, when $DE_E(t_h) < 0$ we pay down-regulation costs, at price χ^-. In both cases, we additionally consider the price-to-pay for the frequency containment reserves, denoted as χ_C. We use Fingrid's data ([20]), and specifically, we apply the average values of the last three months of 2018 equal to $\chi^+ = 56.22$ €/MWh, $\chi^- = 45.97$ €/MWh, $\chi^C = 18.10$ €/MWh. Thus, the cost at t_h is:

$$DP_{Cost}(t_h) = \big|\max\{\chi^+ \cdot DE_E(t_h), \chi^- \cdot DE_E(t_h)\}\big| + \Delta t_r \cdot \chi^C \sum_{t_r = t_h/\Delta t_r}^{t_h/\Delta t_r + 1/\Delta t_r} |DP_E(t_r)|. \quad (19)$$

Assume $\overline{T}$ hours of grid control in total. We define the average dispatch plan energy error per day, CDE_E and the corresponding cost per day, CDP_{Cost}, as:

$$CDE_E = \frac{24}{\overline{T}} \sum_{t_h=0}^{\overline{T}-1} |DE_E(t_h)|, \; CDP_{Cost} = \frac{24}{\overline{T}} \sum_{t_h=0}^{\overline{T}-1} DP_{Cost}(t_h). \quad (20)$$

We assign $w_1 = w_2 = w_3 = w_4 = w_6 = 1$, $w_5 = 10$ and $a_B = 0.1$. w_5 is chosen much larger than the rest of the weights to emphasize on the importance of obtaining a dispatch plan that can be followed by all scenarios. Also, $\underline{\mathrm{E}}_{B,\ell} = 15\%\overline{\mathrm{SoE}}_{B,\ell}$ MWh and $\overline{\mathrm{E}}_{B,\ell} = 85\%\overline{\mathrm{SoE}}_{B,\ell}$ MWh, $\ell \in \{34, 35\}$. For the sixth term in the Eq. (14), let $\mathcal{I}_1$ include the virtual node 34 and the buses with IDs $1-21$, and $\mathcal{I}_2$ include the virtual node 35 and the buses with IDs $22-33$. In all cases, we set $T_{fixed} = 1$ since CoDistFlow takes a few minutes to run for the grid considered in this application, at each iteration of the RHC. Finally, the real-time control algorithm minimizes the error in following the dispatch plan. Also, it does not discharge/charge a battery more than 10%/90% of its capacity.

A. Day-ahead and intra-day forecasts

This section describes the computation of forecasts and forecast scenarios. Although not a contribution of this paper, their availability is essential to evaluate the performance of the proposed re-dispatching strategy. The forecasting engine is based on an ARMA model. The order of the autoregressive and moving average terms are respectively chosen by evaluating the partial autocorrelation and autocorrelation functions, according to conventional practices for their identification. They are 36 (with non-zero coefficients at lags 1, 24, 25 and 36) and 4. Differentiating the time series at lag 1 and 24 was also tested, but it did not contribute to improving the estimation performance. The order of ARMA models at the various buses is the same, but their parameters are estimated for each bus individually. ARMA models are used to generate point predictions for the horizon $1-25$ hours, which are updated in a rolling horizon every 2 hours. Moreover, the variance of the point predictions is used to build parametric probabilistic forecasts in the form of probability density functions (PDFs).

Forecast scenarios are generated with the method described in [9], briefly summarized hereafter for clarity. It relies on the intuition that, if predicted PDFs are reliable, calculating the values of the PDF for the realizations lead to uniformly distributed series, which can be transformed in Gaussian multivariate random variables (i.e., by applying the profit function) and tracked by identifying the associated covariance matrix. The covariance matrix is then used to generate multivariate Gaussian distributed scenarios with off-the-shelf libraries (e.g., `mvnrnd` in Matlab). The random sequences are transformed in the final forecast scenarios by, first, applying the inverse probit function and, finally, the inverse predicted PDFs. Temperature is not considered as a regressor since, in this case, there are no electric-thermal loads.

B. Evaluation of RHC over CoDistFlow on Real Data Sets

Our evaluation is based on historical data from the considered real grid for 10 days ($\overline{T} = 240$). The measurements are used for deriving day-ahead and intra-day forecasts and scenarios (Section VI-A) as well as realizations to which the real-time control algorithm applies. For RHC, we examined different values of the parameter $\Delta\tau$. The results are shown in Fig. 4 and in Table I.

Table I compares the CDE_E and CDP_{Cost} values, as well as the characteristics of the DE_E values among all schemes. Re-dispatch via RHC reduces significantly the error

in following the dispatch plan in real-time. Specifically, if using RHC with $\Delta\tau = 6$ h, CDE_E reduces more than 4.5 times. When $\Delta\tau = 4$ h, CDE_E reduces more than 32.5 times and with $\Delta\tau = 2$ h, it reduces drastically being almost zero. Moreover, the 98% percentile of DE_E is drastically reduced; if $\Delta\tau = 4$ h or lower, it becomes very close to zero. CDP_{Cost} shows the same trends with CDE_E. Notice that no re-dispatching may lead to significant costs along time and across multiple feeders (here, we account for a single feeder). For example, for a single feeder, the expected yearly cost is $24,696$ € compared to 799.2 € that it would have been if re-dispatching every 4 hours. If considering that a small city, such as Lausanne with $150,000$ inhabitants, has $50-60$ feeders, this cost may reach $1,234,800 - 1,481,760$ €, which is a way larger than a cost of $39,960 - 47,952$ € if re-dispatching with $\Delta\tau = 4$ h.

TABLE I: Comparisons of CDE_E, DE_E [kWh], CDP_{Cost} [€].

Scheme	CDE_E	98% perc. DE_E	CDP_{Cost}
No Re-dispatch	978.8	400.91	68.6
$\Delta\tau = 6$ h	209.53	249.51	15.57
$\Delta\tau = 4$ h	29.95	0.0325	2.22
$\Delta\tau = 2$ h	0.15	0.0242	0.0095

Fig. 4(a) shows the DP_E values for all real-time intervals, for schemes without and with re-dispatch. Re-dispatch reduces the number of real-time intervals that dispatch plan tracking fails. In Fig. 4(b), we compare the cdf of DP_E for all schemes. The maximum value of DP_E over all real-time intervals decreases significantly with re-dispatch. For No Re-dispatch it is equal to 736.39 kW and for Re-dispatch it is 453.64 kW with $\Delta\tau = 6$ h, 405.24 kW with $\Delta\tau = 4$ h and 0.365 kW with $\Delta\tau = 2$ h. Thus, if re-dispatching the required power capacity reserves are smaller.

In Figs. 4(c)-4(f), for better illustration purposes, we focus on times between $t_r = 800$ and $t_r = 960$. Figs. 4(c), 4(d) compare the dispatch plan and the realized power, P_1, at the PCC without and with re-dispatch. By comparing Fig. 4(a) with Figs. 4(c), 4(d), we observe that the error is just one order of magnitude smaller than the PCC power and therefore it is important to reduce it via re-dispatching. Indeed, we observe once more that RHC can track the dispatch plan more accurately. Finally, failures in following the dispatch plan are due to depleting the flexibility of the batteries. Figs. 4(e), 4(f) present the SoE of the batteries at the virtual nodes 34 and 35. When the batteries are both full and the generation is greater than the consumption or when they are both empty and the consumption is greater than the generation, there is a failure in following the dispatch plan.

Next, we vary the number of scenarios, D, and study the impact on time complexity and performance of RHC over CoDistFlow. Time complexity refers to the time that CoDistFlow requires to compute an updated S^{DP} at an RHC iteration and does not depend on $\Delta\tau$. We observe that the time complexity increases with the number of scenarios. In the cases examined it is less than 10 min; that is why we choose $T_{fixed} = 1$ that corresponds to 15 min. As a result, re-dispatching every 2 hours for eliminating error and cost (Table I) is totally possible as far as time complexity is considered. In general, the error values, CDE_E, are smaller for larger D. However, introducing re-dispatch leads to a much larger improvement in CDE_E than increasing the number of scenarios of the No Re-dispatch scheme.

TABLE II: Comparisons w.r.t. the number of scenarios.

D	CDE_E [kWh] $\Delta\tau = 6$	CDE_E [kWh] No Re-dispatch	Time complexity (min)
5	300.44	1032	0.35
15	236.4	996.92	1.3
30	234.37	992.01	4
50	223.78	987.41	6
80	209.53	978.8	9

C. Study of RHC over CoDistFlow with Varying Battery Size

In this part, we evaluate the impact of battery capacity on re-dispatching. The battery positions remain the same. Here, we consider $D = 30$ scenarios. Table III shows the results. The CDE_E values decrease as the battery capacity increases, as expected, since a larger battery provides more flexibility to both the day-ahead and the real-time control algorithms.

Re-dispatching via RHC further reduces CDE_E for larger battery capacities. In detail, for small battery capacities, i.e., second and third column of Table III, re-dispatch with $\Delta\tau = 6$ h reduces the CDE_E by $30\% - 64\%$. For larger battery capacities (last two columns of Table III), it reduces the CDE_E by 80%. Therefore, re-dispatch via RHC always improves the battery usage and allows efficiently tracking the dispatch plan with more advantages though for larger battery capacities.

TABLE III: CDE_E values [kWh] for diverse battery capacities. The first line is the per battery capacity (three-phase). Note that in Section VI-B, each battery has a capacity of 3 MWh.

Scheme/Bat. size	0.75 MWh	1.5 MWh	3 MWh	4.5 MWh
No Re-dispatch	2,452	1,703.9	992.01	615.06
$\Delta\tau = 6$ h	1,714	608.22	234.37	108.28

D. Efficiency of using CoDistFlow for Re-dispatch

As mentioned in Section V, by using CoDistFlow we ensure that at convergence the obtained solution satisfies the exact (AC) power flow equations and the exact operational constraints (i.e., Eqs. (1)-(13)). Notably, via our evaluations we verified that the computational complexity required for CoDistFlow is suitable for the re-dispatch time-scale (i.e., every $\Delta\tau$) and that CoDistFlow converges in a few iterations, usually 2 to 5.

We further evaluate the result of the first iteration ($k = 0$) of CoDistFlow in two options, namely, (A) we apply the dispatch plan obtained for $k = 0$, after adding to it the aggregated for all lines at PCC grid and battery losses (computed via LF) for each time interval, (B) we apply the dispatch plan obtained for $k = 0$ (i.e., we do not account for the grid/battery losses). However, the solution obtained at each τ, in both options, will not satisfy the exact power flow equations and operational constraints; note that the battery trajectories, i.e., s_B, are not updated after considering the losses in option (A). For Re-dispatch, we set $\Delta_\tau = 6$ h.

From Table IV, we observe that by ignoring the grid/battery losses (i.e., in option (B)) the CDE_E values increase compared to CoDistFlow (similar results are shown in [6]). In addition, option (A) has very similar CDE_E values as option (B), implying that iterations are important. If considering the city of Lausanne as in Section VI-B, the yearly cost due

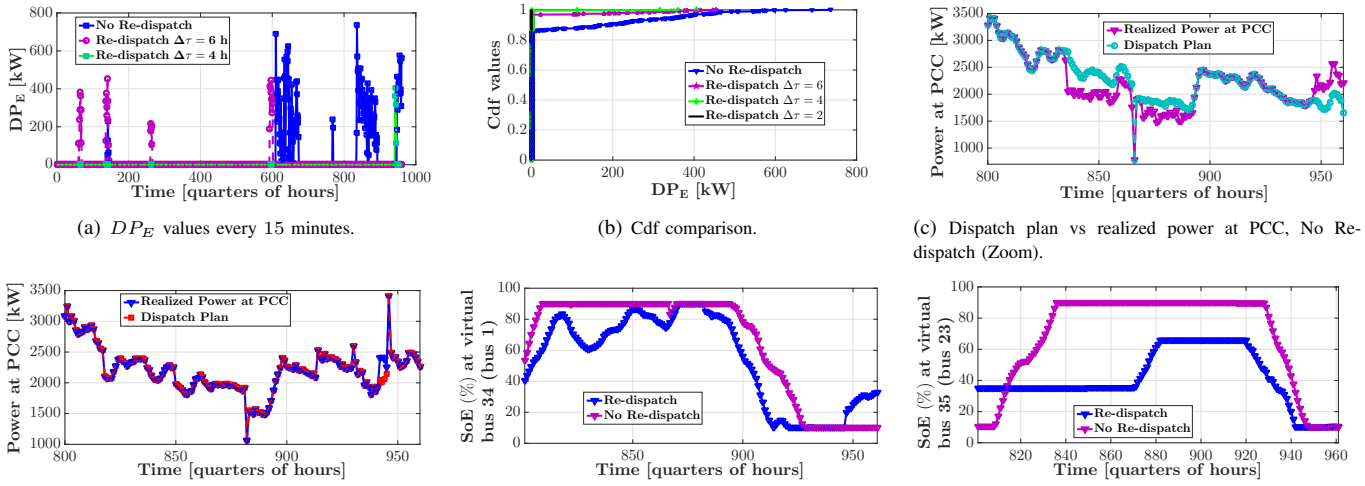

(a) DP_E values every 15 minutes.

(b) Cdf comparison.

(c) Dispatch plan vs realized power at PCC, No Re-dispatch (Zoom).

(d) Dispatch plan vs realized power at PCC, Re-dispatch (Zoom).

(e) State-of-energy (%) at bus 1 (Zoom).

(f) State-of-energy (%) at bus 23 (Zoom).

Fig. 4: State-of-energy and dispatch plan error comparisons. RHC is with $\Delta\tau = 4$ h.

to impossibility of tracking the dispatch plan may have an increase of up to $108,000$ €, when not accounting for the losses both for Re-dispatch and No Re-dispatch.

TABLE IV: CoDistFlow vs. No iterations. CDE_E in kWh, CDP_{Cost} in €.

Scheme	CDE_E Re-disp.	CDP_{Cost} Re-disp.	CDE_E No Re-disp.	CDP_{Cost} No Re-disp.
CoDistFlow	209.53	15.57	978.8	68.6
(A)	270.11	20.07	1031.3	72.9
(B)	270.83	20.13	1032.3	72.98

VII. Conclusions

We proposed and evaluated RHC over CoDistFlow, a re-dispatch scheme for distribution grids with DERs and batteries. The dispatch plan is updated during the grid operation with a receding horizon policy. The update of the dispatch plan is performed via CoDistFlow that efficiently accounts for the grid/battery losses and the grid constraints. The evaluations are performed on a real Swiss grid using real data. We have shown that, if we do not re-dispatch, the daily dispatch plan tracking error and associated cost may become considerably large. On the contrary, if re-dispatching every 6 h, the daily dispatch plan tracking error and associated cost reduce by around 80%, if re-dispatching every 4 h they can reduce more than $30\times$ and if re-dispatching every 2 h they eliminate to zero.

References

[1] R. Lueken and J. Apt, "The Effects of Bulk Electricity Storage on the PJM Market," *Energy Systems*, vol. 5, no. 4, pp. 677–704, 2014.

[2] A. Preskill and D. Callaway, "How Much Energy Storage do Modern Power Systems Need?" *arXiv preprint arXiv:1805.05115*, 2018.

[3] M. Bozorg, F. Sossan, J.-Y. L. Boudec, and M. Paolone, "Influencing the Bulk Power System Reserve by Dispatching Power Distribution Networks Using Local Energy Storage," *Electric Power Systems Research*, vol. 163, pp. 270 – 279, 2018.

[4] J. Leadbetter and L. Swan, "Battery Storage System for Residential Electricity Peak Demand Shaving," *Energy and Buildings*, vol. 55, pp. 685 – 692, 2012.

[5] P. Fortenbacher, J. L. Mathieu, and G. Andersson, "Modeling and Optimal Operation of Distributed Battery Storage in Low Voltage Grids," *IEEE Trans. on Power Systems*, vol. 32, no. 6, pp. 4340–4350, Nov 2017.

[6] E. Stai, L. Reyes-Chamorro, F. Sossan, J. Y. L. Boudec, and M. Paolone, "Dispatching Stochastic Heterogeneous Resources Accounting for Grid and Battery Losses," *IEEE Transactions on Smart Grid*, vol. 9, no. 6, pp. 6522–6539, Nov. 2018.

[7] F. Sossan, E. Namor, R. Cherkaoui, and M. Paolone, "Achieving the Dispatchability of Distribution Feeders Through Prosumers Data Driven Forecasting and Model Predictive Control of Electrochemical Storage," *IEEE Trans. on Sustainable Energy*, vol. 7, no. 4, pp. 1762–1777, 2016.

[8] R. Gupta, F. Sossan, E. Scolari, E. Namor, L. Fabietti, C. Jones, and M. Paolone, "An ADMM-based Coordination and Control Strategy for PV and Storage to Dispatch Stochastic Prosumers: Theory and Experimental Validation," in *Power Systems Computation Conference (PSCC)*, 2018.

[9] P. Pinson, H. Madsen, H. A. Nielsen, G. Papaefthymiou, and B. Klockl, "From Probabilistic Forecasts to Statistical Scenarios of Short-Term Wind Power Production," *Wind Energy*, vol. 12, no. 1, pp. 51–62, 2009.

[10] P. Patrinos, S. Trimboli, and A. Bemporad, "Stochastic MPC for Real-time Market-based Optimal Power Dispatch," in *50th IEEE Conf. on Decision and Control and European Control Conf.*, Dec 2011.

[11] N. Li, L. Chen, and S. H. Low, "Exact Convex Relaxation of OPF for Radial Networks Using Branch Flow Model," in *IEEE Int'l Conf. on Smart Grid Com.*, Nov 2012, pp. 7–12.

[12] M. Nick, R. Cherkaoui, J. L. Boudec, and M. Paolone, "An Exact Convex Formulation of the Optimal Power Flow in Radial Distribution Networks Including Transverse Components," *IEEE Transactions on Automatic Control*, vol. 63, no. 3, pp. 682–697, March 2018.

[13] Y. Ding, M. Xie, Q. Wu, and J. Ostergaard, "Development of Energy and Reserve Pre-dispatch and Re-dispatch Models for Real-time Price Risk and Reliability Assessment," *IET Generation, Transmission Distribution*, vol. 8, no. 7, pp. 1338–1345, 2014.

[14] C. Hamon, M. Perninge, and L. Soder, "The Value of Using Chance-constrained Optimal Power Flows for Generation Re-dispatch Under Uncertainty with Detailed Security Constraints," in *IEEE PES Asia-Pacific Power and Energy Engin. Conf. (APPEEC)*, Dec 2013, pp. 1–6.

[15] C. A. Hans, P. Sopasakis, A. Bemporad, J. Raisch, and C. Reincke-Collon, "Scenario-based Model Predictive Operation Control of Islanded Microgrids," in *54th IEEE Conference on Decision and Control (CDC)*, Dec 2015, pp. 3272–3277.

[16] H. Ding, Z. Hu, and Y. Song, "Rolling Optimization of Wind Farm and Energy Storage System in Electricity Markets," *IEEE Transactions on Power Systems*, vol. 30, no. 5, pp. 2676–2684, 2015.

[17] A. Nottrott, J. Kleissl, and B. Washom, "Storage Dispatch Optimization for Grid-connected Combined Photovoltaic-Battery Storage Systems," in *IEEE Power and Energy Society General Meeting*, 2012, pp. 1–7.

[18] A. Parisio, E. Rikos, and L. Glielmo, "A Model Predictive Control Approach to Microgrid Operation Optimization," *IEEE Transactions on Control Systems Technology*, vol. 22, no. 5, pp. 1813–1827, 2014.

[19] R. Palma-Behnke, C. Benavides, F. Lanas, B. Severino, L. Reyes, J. Llanos, and D. Sáez, "A Microgrid Energy Management System Based on the Rolling Horizon Strategy," *IEEE Transactions on Smart Grid*, vol. 4, no. 2, pp. 996–1006, 2013.

[20] Fingrid, "Reserve Market Information," 2019. [Online]. Available: https://www.fingrid.fi/en/electricity-market/reserves_and_balancing/reserve-market-information, (Accessed: 22/01/2019)